Longitudinal solitons in carbon nanotubes

T. Yu. Astakhova,[1] O. D. Gurin,[1] M. Menon,[2,3,*] and G. A. Vinogradov[1,†]

[1]*Institute of Biochemical Physics RAS, ul.Kosygina 4, Moscow 117334, Russia*
[2]*Department of Physics and Astronomy, University of Kentucky, Lexington, Kentucky 40506-0055*
[3]*Center for Computational Sciences, University of Kentucky, Lexington, Kentucky 40506-0045*

We present results on soliton excitations in carbon nanotubes (CNT's) using Brenner's many-body potential. Our numerical simulations demonstrate high soliton stability in (10,10) CNT's. The interactions of solitons and solitary excitation with CNT defect are found to be inelastic if the excitations and defects length scales are comparable, resulting in a substantial part of soliton energy being distributed inhomogeneously over the defect bonds. In these solitary-excitation–cap collisions the local energy of a few bonds in the cap can exceed the average energy by an order of magnitude and more. This phenomenon, denoted the ''Tsunami effect,'' can contribute dynamically to the recently proposed ''kinky chemistry.'' We also present results of changes in the local density of states and variations in the atomic partial charges estimated at different time instants of the solitary-excitation Tsunami at the nanotube cap.

I. INTRODUCTION

Since the discovery of carbon nanotubes by Iijima,[1] a rich variety of carbon nanotube morphologies has been experimentally observed. Carbon nanotubes (CNT's) are very intriguing objects for both experimental and theoretical investigations due to the many unusual properties they exhibit. Their potential for practical applications, especially in the area of nanotechnology, is very promising. Among their many uses envisioned are applications of nanoscale electronic devices, field-emission displays, and quantum wires.[2] Nanotube doping and structure modification can result in the formation of heterojunctions,[3] diodes,[4] quantum dots,[5] field-effect transistors[6] and one-electron conductors.[7]

The dynamical properties of carbon nanotubes are of great interest due to their potential for useful practical applications.[8] The theoretical methods for explaining these properties range from accurate *ab initio* methods to approximate empirical schemes. Few experimental findings, however, were analyzed using empirical methods that explicitly take into account harmonic contributions such as effects of different vibrational modes. In particular, nonlinear localized excitations can transfer energy and be involved in various processes of interest. There have been some speculations on the role played by solitary excitations in heat transfer, polymer destruction, and other processes occurring in molecular systems.[9] While in most cases of interest the harmonic approximation is sufficient to describe molecular processes, some molecular materials contain atoms interacting through nonlinear interatomic potentials that can give rise to soliton excitations. The investigation of these nonlinear effects is therefore interesting and timely.

In this work we investigate the nonlinear effects in carbon nanotubes giving rise to solitons using empirical methods. We employ Brenner's nonlocal many-body potential for carbon systems.[10] Its simple analytical form as well as its reliability for carbon systems coupled with its computational efficiency makes it a natural candidate for such investigations. The nanotube chosen for our simulations is a (10,10)

tube containing 1000–11 000 atoms. The simulations were performed for free, rigid, and capped tube ends. Our investigations include soliton stability, reflection from free and capped CNT ends, and soliton collisions as well as the influence of thermal fluctuations. We find that the interaction of solitary excitations with the CNT cap can be either elastic or inelastic. In the latter case some part of the energy is retained as an internal excitation of the cap with the remaining portion distributed very inhomogeneously over the C-C bonds. This effect is found to be most pronounced for the nonsymmetrical caps. The degree of energy concentration depends sensitively on the cap structure and solitary-excitation energy and profile. In some cases the energy of few bonds in the cap exceeds the average solitary-excitation energy by an order of magnitude or more. A similar phenomenon is also observed for other defects in CNT's.

The paper is organized as follows: In Sec. II we derive a nonlinear expansion of the Brenner's potential for longitudinal and radial atomic displacements. Section III contains the formulation of an analytical equation for the longitudinal displacements of atoms along the CNT axis. In this section we derive the one-dimensional Korteweg–de Vries equation assuming angular homogeneity and neglecting the radial displacements and obtain the corresponding supersonic soliton solution. Results of the numerical simulations of soliton behavior in CNT's are given in Sec. IV. Section V contains a detailed analysis of solitary-excitation collisions with CNT defects. The possible soliton contributions to various chemical and physical properties of CNT's are briefly discussed in Sec. VI with special attention paid to the changes in the local density of states and variations in partial atomic charges at different instances of the soliton-cap interaction. Along with summarizing our results, we also propose possible ways of soliton generation in this section.

II. NONLINEAR EXPANSION OF THE BRENNER POTENTIAL

Carbon nanotubes (only single-walled CNT's are considered in this work) are highly anisotropic and ordered objects

with great aspect ratio. The CNT surface is formed by a graphitic sheet folded into a cylinder with bond lengths and angles differing slightly from graphite on account of the strain induced by the folding. The interatomic C-C potential is highly unharmonic and can be approximated using classical many-body potentials containing either exponential or power terms. Generally, these potentials do not provide an exactly solvable dynamical equation in the nonlinear continuum approximation, and therefore some approximations need to be made in order to yield desired solutions.

The unharmonic solutions in nonlinear one-dimensional (1D) lattices are frequently approximated by the Korteweg–de Vries (KdV) equation.[12] Since CNT's are quasi-1D objects, in order to obtain nonlinear excitations in CNT's, it is reasonable to approximate a CNT as a 1D lattice with a nonlinear effective potential. We then make the continuum approximation for this system and derive the corresponding KdV equation.

We obtain the nonlinear effective potential for CNT's by expanding Brenner's many-body potential in a Taylor series up to the third-order terms. The corresponding Newtonian equations of motion in finite differences are then derived and finally, the continuous analog (nonlinear partial differential equation) for the system is obtained. This results in a KdV equation that describes longitudinal nonlinear excitations (solitons) in CNT's.

According to Brenner's many-body potential,[10] the bond energy between adjacent atoms i and j is expressed as

$$E_{ij}^b = V_{ij}^R - \bar{B}_{ij} V_{ij}^A, \qquad (1)$$

where V_{ij}^R and V_{ij}^A are, respectively, exponential repulsive and attractive terms: $V^R(r_{ij}) = 27.27 \exp[-3.28(r_{ij} - 1.39)]$ and $V^A(r_{ij}) = 33.27 \exp[-2.69(r_{ij} - 1.39)]$. $\bar{B}_{ij}$ represents an environment-dependent many-body coupling between atoms i and j containing geometric information associated with the system.[10] The total energy of the system is obtained by summing Eq. (1) over all bonds. The energy and distances are measured in eV and angströms, respectively.

The reliability of Brenner's potential has been demonstrated in many numerical calculations of carbon systems in different phases (graphite, diamond, fullerenes, and large clusters), in both the ground state as well as in nonequilibrium states including chemical reactions.[11] Furthermore, the simple form of the potential allows us to easily derive analytical expressions for forces. This also allows efficient large-scale simulations of the system using available computer resources.

In the present work we consider only armchair (m,m) CNT's. The procedure and results are similar in the case of zigzag $(m,0)$ nanotubes. We use the cylindrical coordinate system (R, Φ, Z) for obvious reasons and align the tube axis along the z axis (Fig. 1). With this choice there are $2m$ atoms in the CNT layer having the same z coordinates. The equilibrium distance between layers, l_0, has a slight dependence on the CNT diameter (see Table I). For a (10,10) tube, $l_0 \approx 1.26$ Å.

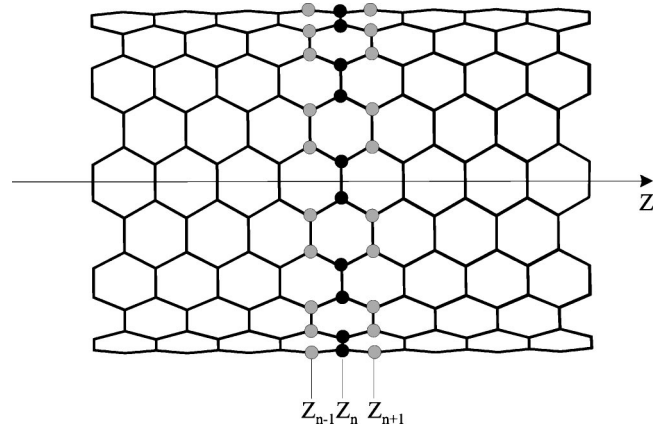Let us consider a cylindrically symmetrical disturbance in the CNT geometry in which all $2m$ atoms in the nth layer

FIG. 1. A part of (10,10) nanotube. The tube is oriented along the z axis. Atoms in nth, $(n \pm 1)$th layers are marked by black and gray circles, respectively.

have identical z and radial displacements from their equilibrium positions Z_n^0 and R^0: $Z_n = Z_n^0 + \zeta_n$ and $R_n = R^0 + \rho_n$, where Z_n and R_n are the perturbed coordinates and ζ_n and ρ_n are the displacements from the equilibrium. Then, the coordinates of ith atom in nth layer are $(R^0 + \rho_n, \quad \Phi_i^0, \quad Z_n^0 + \zeta_n)$. If ζ and ρ are much smaller when compared to characteristic length scales ($\zeta_n \ll l_0$ and $\rho_n \ll R^0$), then the interatomic potential [Eq. (1)] can be expanded in a Taylor series and the terms up to the third order retained:

$$E = E_0 + \sum_{n=1}^{N_l} E_n, \qquad (2)$$

where E_0 is the ground state energy of the relaxed CNT and the perturbation energy is the sum over all N_l layers of CNT's. For every layer $E_n = 2m E_n^a$ is the sum of perturbation energies of $2m$ atoms in the nth layer due to atomic displacements, and the energy of an atom is $E_n^a = \frac{1}{2}(E_1 + E_2 + E_3)$, where E_1, E_2, and E_3 are energies of bonds emerging from any atom in the nth layer (see Fig. 1). It is convenient to reduce both ζ and ρ to dimensionless units: $\zeta_n \to \zeta_n/l_0$, $\rho_n \to \rho_n/l_0$.

TABLE I. Coefficients (in eV) in the expansion of Brenner's potential [Eq. (3)] and the equilibrium distance between layers l_0 (in Å) for CNT's of different diameters.

	(5,5)	(10,10)	(15,15)	(20,20)
a_1	102.80	102.76	102.70	102.66
a_2	296.46	296.22	295.86	294.39
b_1	11.80	2.98	1.32	0.76
b_2	0.34	0.10	0.04	0.00
b_3	9.06	4.59	3.09	2.31
b_4	18.42	2.40	0.72	0.30
c_1	12.24	6.16	4.14	3.10
c_2	71.34	35.82	24.06	17.94
c_3	152.40	154.56	154.20	153.66
l_0	1.2601	1.2573	1.2568	1.2565

Then an expansion E_n^a over atomic ζ and ρ displacements in the nth layer has the form

$$E_n^a = \frac{a_1}{2}(\zeta_{n+1} - \zeta_n)^2 - \frac{a_2}{3}(\zeta_{n+1} - \zeta_n)^3 + \frac{b_1}{2}\rho_n^2$$

$$+ \frac{b_2}{2}(\rho_{n+1} + \rho_n)^2 + \frac{b_3}{3}(\rho_{n+1} - \rho_n)^2(\rho_{n+1} + \rho_n)$$

$$- \frac{b_4}{3}\rho_n^3 + \frac{c_1}{2}(\zeta_{n+1} - \zeta_n)(\rho_{n+1} + \rho_n)$$

$$- \frac{c_2}{3}(\zeta_{n+1} - \zeta_n)^2(\rho_{n+1} + \rho_n) + \frac{c_3}{3}(\zeta_{n+1} - \zeta_n)$$

$$\times (\rho_{n+1} - \rho_n)^2. \tag{3}$$

Numerical values for the expansion coefficients in Eq. (3) are given in Table I for $(5,5),(10,10),(15,15),$ and $(20,20)$ nanotubes. All coefficients in Eq. (3) are measured in eV and variables ζ and ρ are chosen to be dimensionless. Here only the leading terms in the nearest-neighbor interaction are retained. In this assumption the CNT is treated as a one-dimensional lattice with $2m$ carbon atoms at each lattice site interacting through an effective potential given by Eq. (3).

Terms in Eq. (3) can be categorized in three groups. The first contains only longitudinal variables ζ, the second contains only the radial variables ρ, and the third contains cross terms. The coefficients a_1, a_2 in the first group have the largest absolute values and are mostly independent on the CNT diameter (see Table I). The coefficients in other groups (b_i and c_i) have smaller numerical values but a strong dependence on the CNT diameter: the larger the CNT diameter, the smaller the values of these coefficients. This indicates that the contribution from the longitudinal degree of freedom to the dynamical properties of CNT is dominant, and the role of other members decreases with the increase in the CNT diameters. We therefore consider only the longitudinal degree of freedom in the study of nonlinear dynamics. Analytical and numerical results for the case in which both longitudinal and radial degrees of freedom are considered will follow in a future report. We note that these results differ only in minor quantitative details, the main features being determined by the longitudinal degree of freedom.

Note that the oscillatory equation for the radial vibrations

$$M\frac{\partial^2 \rho_n}{\partial t^2} = -b_1 \rho_n$$

gives the lowest-frequency "breathing" mode in the harmonic radial approximation for CNT's, and the Raman frequency for this mode for the (10,10) CNT is ≈ 165 cm^{-1}, where M is the mass of carbon atom.

The Newtonian equation of motion for longitudinal ζ displacements (neglecting radial degrees of freedom) is

$$M\frac{\partial^2 \zeta_n}{\partial t^2} = a_1[(\zeta_{n+1} - \zeta_n) - (\zeta_n - \zeta_{n-1})]$$

$$- a_2[(\zeta_{n+1} - \zeta_n)^2 - (\zeta_n - \zeta_{n-1})^2]. \tag{4}$$

This is a nonlinear equation in finite differences. In the next section we derive its continuum analog and examine the consequences.

III. KORTEWEG–DE VRIES SOLITONS IN CNT'S

Equation (4) presents a true 1D nonlinear problem with only one variable ζ. The corresponding continuum equation is obtained by using the work of Toda.[13] Let the relative displacement of all atoms in nth and $(n-1)$th layers be given by $\chi_n = \zeta_n - \zeta_{n-1}$. The continuum approximation is then valid if only excitations with wavelengths much greater than the lattice constant l_0 are allowed. The expression for the 1D expansion of Brenner's potential [Eq. (2)] in Taylor series can be written as

$$E = E_0 + \sum_{n=1}^{N_l} \left(\frac{a_1}{2}\chi_n^2 - \frac{a_2}{3}\chi_n^3 \right). \tag{5}$$

The corresponding equation of motions for relative displacements χ is

$$M\frac{\partial^2 \chi_n}{\partial t^2} = 2[a_2\chi_n^2 - a_1\chi_n] - [a_2\chi_{n+1}^2 - a_1\chi_{n+1}]$$

$$- [a_2\chi_{n-1}^2 - a_1\chi_{n-1}]. \tag{6}$$

Equation (6) contains terms with $\chi_{n\pm1}$ and $\chi_{n\pm1}^2$. It is convenient to introduce a shift operator $\mathcal{P}^{\pm1} = \exp(\pm\partial/\partial n)$ for a shift along the discrete chain by one step to the right (left) such that $\mathcal{P}^{\pm1}f(n) = f(n\pm1)$, where $f(n)$ is an arbitrary function of discrete coordinate n. Equation (6) can then be written as

$$M\frac{\partial^2 \chi_n}{\partial t^2} = \left[2 - \exp\left(\frac{\partial}{\partial n}\right) - \exp\left(-\frac{\partial}{\partial n}\right)\right](a_2\chi_n^2 - a_1\chi_n), \tag{7}$$

or

$$M\frac{\partial^2 \chi_n}{\partial t^2} = -\left[2\sinh\left(\frac{1}{2}\frac{\partial}{\partial n}\right)\right]^2 (a_2\chi_n^2 - a_1\chi_n), \tag{8}$$

resulting in

$$M\frac{\partial^2 \chi}{\partial t^2} - a_1\left[2\sinh\left(\frac{1}{2}\frac{\partial}{\partial n}\right)\right]^2\chi + a_2\left[2\sinh\left(\frac{1}{2}\frac{\partial}{\partial n}\right)\right]^2\chi^2 = 0. \tag{9}$$

If $\sinh(\frac{1}{2}\partial/\partial n)$ in the third term in Eq. (9) is expanded in Taylor series up to the linear term, then the equation can be rewritten as

$$M\frac{\partial^2 \chi}{\partial t^2} - a_1\left[2\sinh\left(\frac{1}{2}\frac{\partial}{\partial n}\right)\right]^2\chi + a_2\frac{\partial^2}{\partial n^2}\chi^2 = 0, \tag{10}$$

and can be factored into the following products:

$$\left\{ \sqrt{M} \, \frac{\partial}{\partial t} \mp 2\sqrt{a_1} \sinh\left(\frac{1}{2}\frac{\partial}{\partial n}\right) \pm \frac{a_2}{\sqrt{a_1}}\frac{\partial}{\partial n} \right\}$$

$$\times \left\{ \sqrt{M} \, \frac{\partial}{\partial t} \pm 2\sqrt{a_1} \sinh\left(\frac{1}{2}\frac{\partial}{\partial n}\right) \mp \frac{a_2}{\sqrt{a_1}}\chi\frac{\partial}{\partial n} \right\}\chi = 0.$$

$$(11)$$

Equations (10) and (11) are equivalent modulo terms of third order. Equation (11) has a form of a product of two operators $\hat{F}_1\hat{F}_2\chi$. If we make a further assumption: $\hat{F}_2\chi = 0,$[13] then the wave packet moving to the right (left) is described by

$$\left\{ \sqrt{M} \, \frac{\partial}{\partial t} \pm 2\sqrt{a_1} \sinh\left(\frac{1}{2}\frac{\partial}{\partial n}\right) \mp \frac{a_2}{\sqrt{a_1}}\chi\frac{\partial}{\partial n} \right\}\chi = 0. \quad (12)$$

If $\sinh(\frac{1}{2}\partial/\partial n)$ in Eq. (12) is further expanded in a Taylor series up to the third-order terms and n is substituted by continuum variable z, one gets the corresponding continuum equation:

$$\frac{\partial \chi}{\partial t} + k_1 \frac{\partial \chi}{\partial z} + k_2 \frac{\partial^3 \chi}{\partial z^3} - k_3 \chi \frac{\partial \chi}{\partial z} = 0, \quad (13)$$

where $k_1 = k$, $k_2 = k/24$, $k_3 = (a_2/a_1)k$, and $k = \pm\sqrt{a_1/M}$.

Equation (13) can be reduced to the standard KdV equation ($u_\tau + 6uu_x + u_{xxx} = 0$) by the linear substitution of variables:

$$\delta = k/24, \quad \tau = \delta t, \quad x = z - kt, \quad u = a_2 k\chi/6\delta a_1. \quad (14)$$

Then the soliton solution of Eq. (13) has a form

$$\chi = \pm A \, \text{sech}^2(Bz \pm Ct). \quad (15)$$

Here $A = 12(k_2/k_3)B^2$, $C = B(k_1 + 4k_2B^2)$. Solution of Eq. (15) is a soliton with amplitude A of either compression ($A<0$) or elongation ($A>0$) propagating in the positive or negative direction along the z axis with velocity $v_{sol} = C/B$. It describes a continuum set of one-parametric solitons, i.e., coefficients A and C can be expressed through the single parameter, e.g., soliton half-width $w \approx 1.76/B$.

Soliton velocity can be expressed as $v_{sol} = k_1 + 4k_2B^2 = v_{sound}(1 + 0.52/w^2)$, where $v_{sound} = k_1 = \sqrt{a_1/M}$ is the longitudinal sound velocity (≈ 20 km/sec). This value is in good agreement with the value 20.35 km/sec obtained in Ref. 14. The solution [Eq. (15)] is thus the supersonic soliton. For the solitons used extensively in our numerical simulations (Sec. IV), the value $w = 2$ was usually employed, and $v_{sol} \approx 1.13 v_{sound}$. Note that the solution [Eq. (15)] has a form of solitary wave for *relative z* displacements. For *absolute z* coordinates it transforms into a kink solution $\approx \tanh(Bz \pm Ct)$. In the limit $w \to \infty$ the soliton velocity tends to the sound velocity. The dependence of v_{sol} on w is shown in Fig. 2. Solitons with $w \lesssim 1$ (less than the lattice constant l_0) are highly unstable in discrete systems, and therefore this dependence is shown only for $w \geq 1.5$.
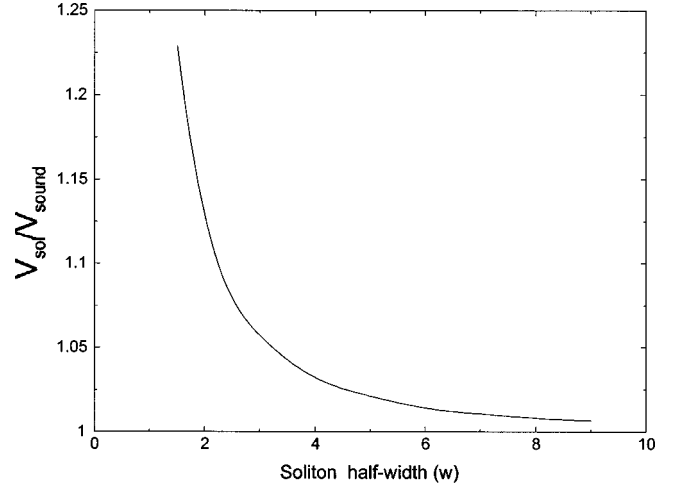

FIG. 2. The dependence of soliton velocity v_{sol} on the soliton half-width w. v_{sound} is the longitudinal sound velocity.

The soliton in Eq. (15) contains both kinetic and potential energies and their contribution to the total energy of soliton (E^{tot}) are roughly the same. The dependence of (E^{tot}) on w as well as individual contributions from kinetic (E^{kin}) and potential (E^{pot}) energies is shown in Fig. 3.

The solution [Eq. (15)] was obtained using rather crude approximations, neglecting higher-order terms in the expansion of Eq. (5) and radial displacements. In order to obtain a more realistic soliton behavior, we next perform detailed numerical simulations.

IV. NUMERICAL SIMULATION OF SOLITONS IN CNT'S

We present our results of the molecular dynamical (MD) simulation using Brenner's many-body potential for the soliton evolution in the (10,10) CNT subject to different boundary conditions that include free, rigid, or capped ends. The findings for the (6,6) CNT are essentially the same.
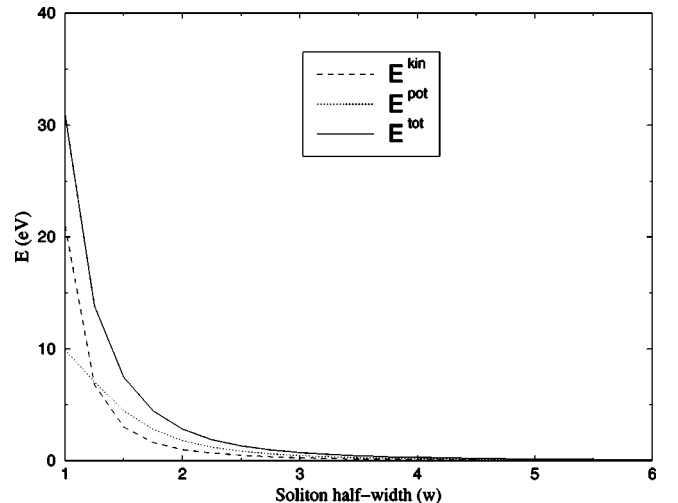

FIG. 3. The dependence of total soliton energy (E^{tot}) on soliton half-width w and individual contributions from kinetic (E^{kin}) and potential (E^{pot}) energies.
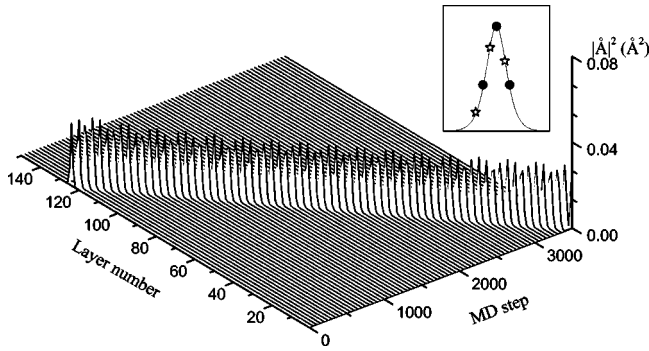
FIG. 4. Soliton evolution in the (10,10) nanotube with 3000 atoms (150 layers) with free ends. The soliton half-width is $w=2$ and $|A|^2 = \chi_n^2$ is the square of relative longitudinal displacements of the nth and $(n-1)$th layers. The modulation of the soliton amplitude in this figure is explained by the lattice discreteness and soliton narrowness. Actual χ values are shown in insertion at two different time instants (labeled by the full circle and empty stars, respectively). Only maximal values of $|A|^2$ reflect the soliton stability.

Our CNT consisted of 1000–11 000 carbon atoms (the number of layers $N_l = 50$–550), with a nanotube length in the range 63–700 Å. The integration MD step was 0.35 fs and the Verlet-Beemann algorithm was used to integrate the equations of motion. Initial conditions were chosen in the form given by Eq. (15) with typical range of parameters values: $w=2$–5, $A=0.2$–0.03 Å.

The solution Eq. (15), describes the compression or elongation soliton with variable amplitudes and velocities depending on the half-width w, propagating on the CNT surface. This solitary excitation is homogeneous with respect to the azimuthal angle Φ. As a first step in the numerical simulation we investigate the soliton evolution in CNT's with frozen radial displacements, i.e., by allowing only the z displacements of the atoms.

The time evolution of a single soliton propagating along the (10,10) nanotube is shown in Fig. 4. The soliton is rather stable as it traverses the CNT length (≈ 150 Å) with only a minimal decrease in amplitude. For CNT's with cyclic boundary conditions the soliton can travel much longer paths without suffering any noticeable decrease in amplitude. The $|A|^2$ value, approximately proportional to the elastic soliton energy in the harmonic approximation, is plotted in Fig. 4. The wider the soliton, the greater its stability. In the limit of infinite CNT diameter, Eq. (15) describes a soliton propagating on the graphite surface. Its behavior is likely to be similar to the soliton in an isotropic hexagonal lattice with the Lennard-Jones interatomic potential, propagating along the $[\bar{1}10]$ direction.[15]

While the soliton with half-width $w<2$ interacts with open CNT ends inelastically, a wider soliton reflects from the open ends without any appreciable changes. Rigid CNT ends, on the other hand, are found to preserve the soliton stability for any w.

The collision of two solitons with different parameters is illustrated in Fig. 5. As seen in the figure, the solitons collide and pass through each other without changing their profiles
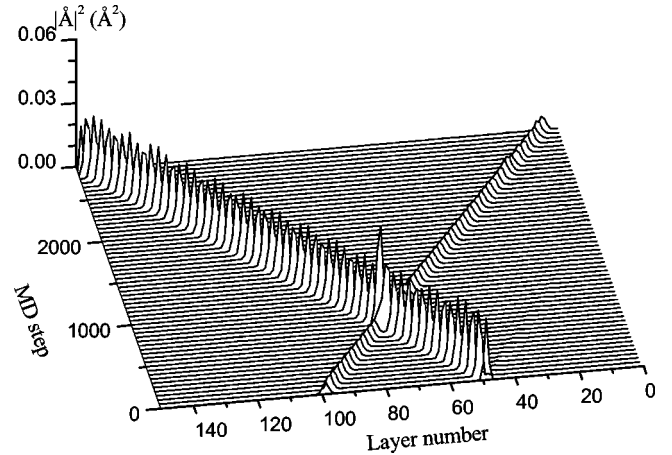

FIG. 5. Temporary evolution of two solitons with $w_1=2$ (right at $t=0$) and $w_2=3$ (left at $t=0$) moving initially toward each other. CNT's and notations are the same as in Fig. 4.

and velocities, demonstrating their characteristic soliton feature.

Our numerical simulations performed at $T=300$ K showed no evidence of the influence of thermal fluctuations on the soliton stability. Also, there were no detectable soliton distortions in the presence of defects (point mass defects, vibrationally excited bonds, etc.) in the CNT structure. Furthermore, no significant interaction with low-intensity Raman-active tangential mode (~ 1585 cm^{-1}) was observed. Results of the MD simulations, therefore, support the fact that the KdV equation is a good approximation for the description of longitudinal nonlinear excitations—solitons in CNT's—if radial displacements are frozen.

We have also performed MD simulations of soliton evolution (propagation, reflection and collision between two solitons) in a 1D lattice (a true 1D analog of CNT) consisting of atoms interacting through the potential described by Eq. (5). Our results are in full agreement with the findings for the CNT's, suggesting that the neglect of higher-order terms in the expansion of Brenner's many-body potential [Eq. (1)] is justified. The situation changes, however, if the radial degrees of freedom are allowed. The folding of the graphite sheet to form CNT's results in the mixing of longitudinal and radial modes. As a result, equations of motion for these two modes now contain cross terms that can influence the behavior of a longitudinal soliton.

The numerical simulation of the initial state evolution chosen in the form of longitudinal soliton in CNT [Eq. (15)] with *all* allowed degrees of freedom shows the soliton to be less stable, with a slow dissipation of the initial energy through the harmonic radial oscillations. Results of analytical analysis and detailed numerical investigations of the longitudinal-radial solitons are planned to be presented in a forthcoming paper.

V. INTERACTION OF SOLITARY EXCITATIONS WITH NANOTUBE CAPS

We next investigate the interaction of the solitons with nanotube caps. Our results for the interaction of narrow (w

$=2-4$) solitons with nonlocal defects (free tube ends and caps) show it to be inelastic with the excitation energy being distributed approximately evenly over all the bonds in this region. Interesting effects can be expected in the case when the length scales of both the excitations and defects are comparable. Towards this end, we perform a detailed numerical investigation of interaction of excitations with the CNT caps.

Solitons with $w=10$ carry too small an energy to induce any noticeable effects in the cap. So we used solitary excitations with other profiles. When a solitary excitation has a characteristic length scale much greater than the lattice constant the nonlinear effects can be ignored and can be treated within the harmonic approximation. Furthermore, for long-wavelength excitations, the dispersion effects in harmonic approximation are not significant. In this case, an arbitrary excitation propagates along the harmonic chain with speeds close to the sound velocity with only a minimal change in its profile. We have examined the propagation of a longitudinal solitary excitation using the parameters $\chi=A\,\mathrm{sech}^2[B(z-v_{\text{sound}}t)]$ with $w=10$ and $A=0.1$ Å. This excitation was found to be highly stable even when all degrees of freedom were allowed and survived the reflection from free ends.

The same results were obtained for solitary waves with other analytical profiles and similar widths and amplitudes. The other types of excitations studied included an excitation of the Gaussian profile

$$\chi=\frac{A}{\sqrt{2\pi}w}\exp\left[-\frac{(z-v_{\text{sound}}t)^2}{2w^2}\right],$$

also with $w=10$ and $A=0.1$ Å.

Although the soliton propagation is accompanied by a highly coherent and predominantly longitudinal displacements of the atoms on the cylindrical surface of the CNT, the atoms on the cap behave quite differently after the solitary-wave–cap collision. When the solitary excitation reaches the cap, there is an accumulation of energy at the cap. Part of the total energy of the solitary wave is likely to be dissipated and/or accumulated on structural defects. We consider an example in which solitary wave interacts with nonsymmetrical caps.

Our simulation of soliton interaction with the nanotube cap consisted of the following sequences: (A) The incoming excitation causes the cap to ''inflate'' with the cap attaining nearly a spherical shape. At this instant the potential energy of the cap attains a maximum value, although the energy distribution in the bonds are unequal due to the asymmetry in the cap. Atoms in the tip of the cap are displaced by ≈ 0.3 Å in the positive z direction. (B) The recoil of the elastic energy of the cap causes atoms to move in the opposite direction and at some instant the kinetic energy attains a maximum value. The velocities of atoms are all predominantly directed along the z axis although they differ significantly from each other in their magnitudes. (C) Atoms at the cap continue to be propelled by inertia and the elastic potential energy attains a maximum again. At this instant, the cap acquires regions with negative curvature, and the displacement of the tip of the cap from its equilibrium position is ≈ -0.8 Å. (D) After this the atoms in the cap start to move
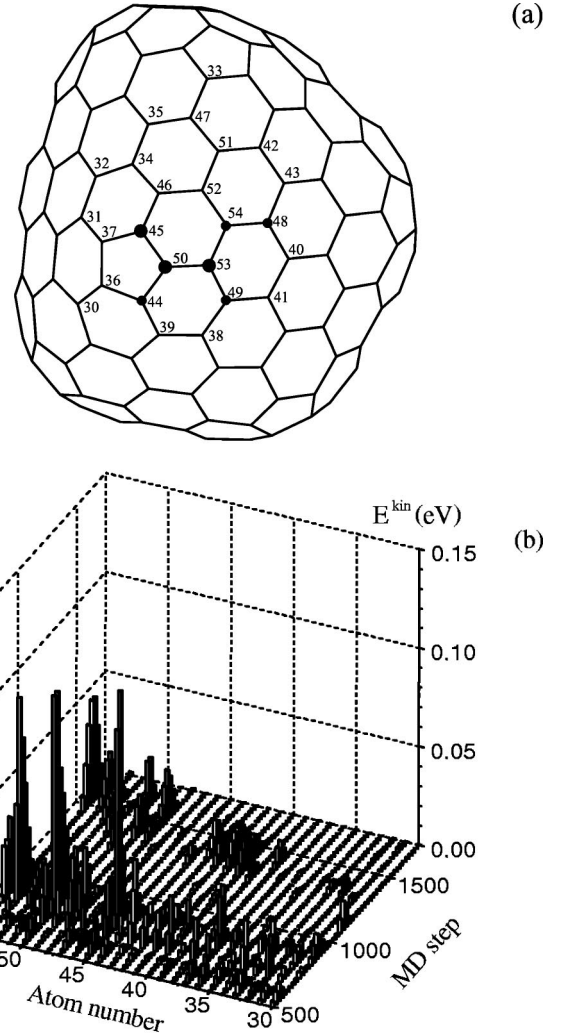

FIG. 6. (a) Schlegel diagram and atomic numbering of the nonsymmetrical (10,10) CNT cap; (b) temporary evolution of the kinetic energy distribution over atoms in the cap. Initial condition: solitary excitation with $w=10$ moves from the tube to the cap and at the $t\approx 600$ MD step reaches the cap. The maximum energy concentration is attained at $t\approx 800$ MD steps.

in the opposite direction toward the equilibrium state and a second, but less intense, maximum in the kinetic energy is observed.

The nanotube cap continues to oscillate with rapidly decreasing amplitude, the energy being dissipated in heating the cap and the CNT ''body.'' Note the large total amplitude of the tip displacements (>1.0 Å). A striking feature of this preliminary result observed in MD simulations is the inhomogeneity of the energy distribution in the cap after the solitary-wave–cap collision. We next investigate the cap dynamics and energy distribution over atoms in more details.

A typical time dependence of the kinetic energy distribution over atoms in the (10,10) cap is shown in Fig. 6(b) as a histogram. The Schlegel diagram of this cap is shown in Fig. 6(a). This cap was chosen from a full list of 9342 topologically different caps with isolated pentagons generated previously.[16] Atom numbering is common to both Figs. 6(a) and 6(b), and atoms with numbers less than 30 (in the cap
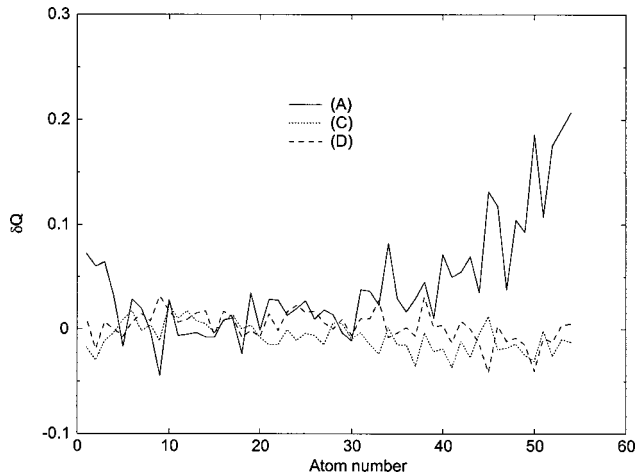
FIG. 7. Variation of the partial Mulliken charges at the cap at different time instants. Atomic numbering is the same as in Fig. 6. (A) largest ''positive'' expansion of the cap [stage (A)]; (C) ''negative'' shrinkage [stage (C)].

FIG. 8. Variation of the densities of states averaged over the cap atoms at different instances. Legends are the same as in Fig. 7.

base) are not shown as they have lower (<0.02 eV) excitation levels. Two ''waves'' of excitations are visible in this figure: one at $t=750-800$ MD steps [stage (B)] and the other with a lower excitation level—at $1300-1600$ MD steps [stage (D)]. The atoms with energy $\geqslant 0.1$ eV are drawn in large circles in Fig. 6(a); atoms with energy $\geqslant 0.05$ eV in medium circles. An excitation area is localized and bears a larger portion of total cap energy. One can see that the kinetic energy is concentrated mainly at the tip of the cap, irrespective of the location of pentagons.

We denote this effect of energy concentration as the ''Tsunami effect'' (named for the effect explaining ocean waves coming to a beach) because initially the long-wavelength and low-amplitude excitation is concentrated into a sharp impulse of energy if the conditions for the solitary-wave propagation are changed in a special manner. It was found that this effect depends on the cap structure and is more pronounced in less symmetrical caps. The effect is observed if the cap radius is comparable with solitary-wave half-width w (in the case shown in Fig. 7 for $w=10$). Otherwise, the Tsunami effect is less prominent. Analogously similar phenomena with varying degrees of perfections were observed for other defects (kinks and bends) in CNT's.

We have also calculated electronic properties of the capped CNT's during the solitary-wave–cap collision using a generalized tight-binding scheme of Menon and Subbaswamy.[17] The variation of the partial Mulliken charge distribution obtained using this scheme is shown in Fig. 7. These calculations were performed for time instants corresponding to the maximal cap distortions [stages (A) and (C)]. The most significant change, as expected, is observed for atoms at the tip of the cap (indicated by large number labels in Fig. 7) where perturbation in the structure is a maximum.

The local electron density of states (DOS) averaged over atoms at the cap at stages (A) through (C) of solitary-wave–cap collision is shown in Fig. 8. The DOS is obtained from the Green's function $G(E)=[ES-H+i\delta]^{-1}$, where H is
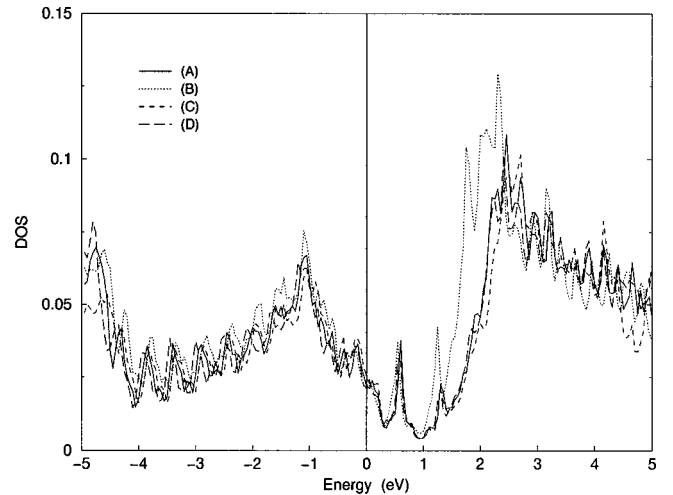
the generalized tight-binding Hamiltonian, S the overlap,[17] and $\delta=0.05$ eV. Note the rather large variations in the DOS.

VI. CONCLUSION

We have thus demonstrated analytically, using numerical simulations, that the KdV solitons are reasonably good approximations for the description of nonlinear excitations in CNT's. The soliton stability increases with the CNT diameter and, in the limit $R\rightarrow\infty$, the solution [Eq. (15)] describes the nonlinear excitations in graphite. Our numerical simulations of the evolution of the initial longitudinal soliton confirms its high stability.

We have also performed numerical simulations of the interaction of solitary-wave excitations (different from solitons) with defects in CNT's, especially with caps (the Tsunami effect). Our simulations show many new fascinating features in the dynamics of CNT's. The collision is found to be partially inelastic, and the cap excitation is highly inhomogeneous. Interestingly, at some instances the energy in a few bonds considerably exceeds the averaged energy of the solitary excitation. This process can provide an extra dynamical contribution to the recently discovered phenomenon of the enhanced reactivity of defect sites in CNT's termed ''kinky chemistry.''[18,19]

The issues concerning methods of soliton excitation in real CNT's and their possible contribution to various chemical and physical phenomena are not yet clear. In reality, the generation of the highly coherent ultrashort longitudinal displacements of atoms in the CNT seems hardly probable. This, however, is not the case for the long-wavelength solitary excitations. In this connection we would like to point out recent results on the optomechanical effect in CNT's.[20,21] Conceivably a short flash of light could trigger the CNT excitation in such a manner that the solitary excitations will be generated. They can also be generated due to external factors such as electron or ion impacts, stress release, and other mechanisms. If solitary excitations do exist in CNT's

in reasonable ''concentration,'' then they can be identified through their contribution to some detectable CNT properties. A possible example is the Tsunami effect when the energy, smoothly distributed in the large-scale excitation of an arbitrary profile, can be concentrated on a few bonds of a defect with considerable energy excess. The greater the distortions in CNT's, the greater this influence. It can also be a way for ''self-healing'' of CNT's when a rearrangement of structural imperfection is activated by solitary excitations. This effect also can promote chemical reactions such as C_2 incorporation into nanotube caps.

The high specific heat of a rope of single-walled nanotube observed[22] can be partially explained by solitary excitations generated in parallel with phonons. Heat transfer in CNT's is another example.[23–25] Emission of short electric field pulses, when the solitary wave inelastically interacts with the non-symmetrical caps or other defect sites, can be yet another example. Our results of the calculation of variation in charge distribution and DOS confirm the large deviation of the electronic properties from their equilibrium values at the solitary-excitation–cap collision. The process of charge distribution variation under dynamical excitation is probably inversely related to the optomechanical phenomenon in CNT's.[20,21] Nanotechnology is one area where the mechano-electric property of CNT's can be used.

Note added. Recently we became aware of a very recent work on solitons by Chamon.[26] In this paper the spontaneous lattice distortions are investigated similar to the case of polyacetylene. The solitons are topological domain walls separating different symmetry-broken vacua with different Kekule bond-alternation structures. Note that the solitons discussed by Chamon and those found in the present work have a different nature: we have considered solitons formed due to the elastic and nonlinear properties of CNT, while the Chamon solution is a topological soliton.

*Electronic address: super250@pop.uky.edu

†Corresponding author. Electronic address: gvin@deom.chph.ras.ru

[1] S. Iijima, Nature (London) **354**, 56 (1991).

[2] *Nanotechnology Research Directions*, edited by M. C. Roco, R. S. Williams, and P. Alivisatos (Kluwer Academic, Dordrecht, the Netherlands, 2000).

[3] Z. Yao, H. Potsma, L. Balents, and C. Dekker, Nature (London) **402**, 273 (1998).

[4] C. Papadopoulos, A. Rakitin, J. Li, A. S. Vedeneev, and J. M. Xu, Phys. Rev. Lett. **85**, 3476 (2000).

[5] R. Tamura and M. Tsukuda, Phys. Rev. B **52**, 6015 (1995); D. L. Carroll, P. Redlich, P. M. Ajayan, J. C. Charlier, X. Blase, A. deVita, and R. Car, Phys. Rev. Lett. **78**, 2811 (1997); P. Kim, T. W. Odom, J.-L. Huang, and C. M. Lieber, *ibid.* **82**, 1225 (1999).

[6] S. J. Tans, A. R. M. Verschueren, and C. Dekker, Nature (London) **393**, 49 (1998); S. J. Tans, A. R. M. Verschueren, and C. Dekker, *ibid.* **404**, 834 (2000); R. Martel, T. Schmidt, H. R. Shea, and T. Hertel, Appl. Phys. Lett. **73**, 2447 (1998).

[7] M. Bockrath, D. H. Cobden, and P. L. McEuen, Science **275**, 1922 (1997).

[8] H. G. Craighead, Science **290**, 1532 (2000).

[9] *Solitons in Action*, edited by K. Lonngren and A. Scott (Academic, New York, 1978).

[10] D. W. Brenner, Phys. Rev. B **42**, 9458 (1990).

[11] Y. Xia, Y. Ma, Y. Mu, C. Tan, and L. Mei, Phys. Rev. B **61**, 11 088 (2000); B. Ni and S. B. Sinnott, *ibid.* **61**, R16 343 (2000).

[12] J. Ford, Phys. Rep. **213**, 271 (1992).

[13] M. Toda, *Theory of Non-linear Lattices* (Springer, Berlin, 1981).

[14] R. Saito, T. Takeya, T. Kimura, G. Dresselhaus, and M. S. Dresselhaus, Phys. Rev. B **57**, 4145 (1998).

[15] Y. Zolotaryuk, A. V. Savin, and P. L. Christiansen, Phys. Rev. B **57**, 14 213 (1998).

[16] T. Yu. Astakhova, G. A. Vinogradov, and E. Osawa, Fullerene Sci. Technol. **7**, 769 (1999); G. Brinkmann, P. W. Fowler, D. E. Manolopoulos, and A. H. R. Palser, Chem. Phys. Lett. **315**, 335 (1999).

[17] M. Menon, E. Richter, and K. R. Subbaswamy, J. Chem. Phys. **104**, 5875 (1996).

[18] D. Srivastava, D. W. Brenner, J. D. Schall, K. D. Ausman, M. F. Yu, and R. S. Ruoff, J. Phys. Chem. B **103**, 4330 (1999).

[19] K. D. Ausman, H. W. Rohrs, M. F. Yu, and R. S. Ruoff, Nanotechnology **10**, 258 (1999).

[20] Y. Zhang and S. Iijima, Phys. Rev. Lett. **82**, 3472 (1999); P. Kral, E. J. Mele, and D. Tomanek, *ibid.* **85**, 1512 (2000).

[21] P. Poncharal, Z. L. Wang, D. Ugarte, and W. A. Deheer, Science **283**, 1513 (1999).

[22] A. Mizel, L. X. Benedict, M. L. Cohen, S. G. Louie, A. Zettl, N. K. Budraa, and W. P. Beyermann, Phys. Rev. B **60**, 3264 (1999).

[23] W. Yi, L. Lu, D. L. Zhang, Z. W. Pan, and S. S. Xie, Phys. Rev. B **59**, R9015 (1999).

[24] J. Hone, M. Whitney, C. Piskoti, and A. Zettl, Phys. Rev. B **59**, R2514 (1999).

[25] S. Berber, Y.-K. Kwon, and D. Tomanek, Phys. Rev. Lett. **84**, 4613 (2000).

[26] C. Chamon, Phys. Rev. B **62**, 2806 (2000).